文章编号: 1001－2060(2007)04－0427－04

荷电颗粒可压缩性颗粒层模型

黄　斌, 姚　强, 龙正伟, 宋　蔷
(清华大学 热能动力工程与热科学教育部重点实验室, 北京 100084)

摘　要: 研究发现荷电颗粒有趋向于沉积在颗粒链尖端的趋势, 据此在已建立的中和可压缩性颗粒层模型中加入荷电颗粒的沉积性质, 建立了荷电颗粒可压缩性颗粒层模型, 从而研究滤料过滤过程中的颗粒层过滤阶段的机理。通过模型发现, 不可压缩时, 荷电颗粒形成的颗粒层的高度与中和颗粒层相似, 但空隙分布均匀; 由于下滑角较小, 其不易被压缩, 当压降增大到一定程度时, 呈周期性压缩, 所以在较高过滤风速下其压降显著低于中和工况。模型结果成功地解释了实验现象。

关　键　词: 荷电颗粒; 颗粒层; 压缩; 压降; 空隙率

中图分类号: X701.2　　文献标识码: A

引　言

越来越苛刻的环保排放标准要求具有更高效的除尘技术, 静电与过滤式除尘器(布袋除尘器和陶瓷体过滤器)相结合的技术得到了广泛的关注。实验已经发现, 荷电颗粒在过滤器表面形成的颗粒层能够获得更低的过滤压降, 但由于直接对颗粒层结构研究的困难性, 一直没有获得对机理的解释。

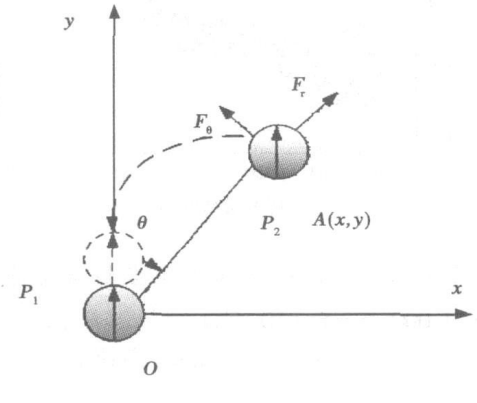

图 1　荷电颗粒在颗粒链尖的沉积

通过实验观察研究发现, 荷电颗粒有在纤维上形成直链的趋势[1], 这主要是荷电颗粒具有的偶极矩与沉积颗粒以及纤维之间的相互作用的结果, 如图 1 所示。作用力可由式(1)和式(2)表示[2]:

$$F_r=\frac{3P_1P_2}{4\pi\varepsilon_0}\frac{1-3\cos^2\theta}{r^4} \tag{1}$$

$$F_\theta=\frac{6P_1P_2}{4\pi\varepsilon_0}\frac{\sin\theta\cos\theta}{r^4} \tag{2}$$

其中: F_r 和 F_θ —颗粒间偶极矩产生的径向和切向作用力; P —颗粒偶极矩; ε_0 —真空电介常数; r —颗粒间距; θ —偶极矩方向与颗粒间连线的夹角。

通过对颗粒间作用力的分析, 中和颗粒的形成模型和可压缩模型已建立[3], 模型成功地模拟了二维的中和颗粒的沉积情况以及压力达到一定时期颗粒层的坍塌行为。

1　荷电颗粒层的形成模型

对于单纤维, 荷电颗粒在颗粒链尖端的沉积可以通过引入式(1)和式(2)模拟得到[3], 但对于颗粒层, 气溶胶颗粒将面对比单纤维更为复杂和庞大的颗粒群, 对其进行完全的模拟很困难, 需要作必要的简化。

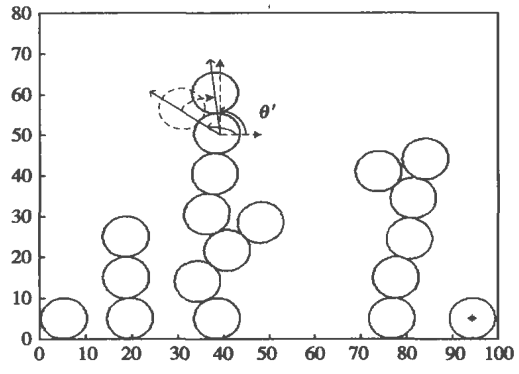

图 2　荷电颗粒层形成模型

收稿日期: 2006－10－08;　修订日期: 2006－12－11
基金项目: 国家"973"基金资助项目(2002CB211600)
作者简介: 黄　斌(1978－), 男(彝族), 云南弥关人, 清华大学博士研究生;

在颗粒层中，气流中的颗粒在接近颗粒层时，由式(1)和式(2)可知，其作用力与距离的四次方成反比，颗粒受到的影响主要来自接近它的那部分，即对于静电作用来说，它只能“看到”颗粒层中的颗粒链，而且在颗粒层上部填充率非常低，所以颗粒也将有可能形成颗粒直链。本研究依此进行简化，对来流的颗粒给一个随机的具有趋向于链顶端的作用，以便认识静电对颗粒层的影响。

模型首先采用已建立的不可压缩颗粒层的形成模型形成颗粒层，沉积到颗粒簇上的颗粒与其接触颗粒的角度为 θ，然后沿其接触的颗粒给出$[0, \pi/2]$的随机数，如图 2 所示，其角度 θ'变为：

$$\theta' = \theta + (\pi/2 - \theta)\sin(\mathrm{rand}(\pi/2)) \quad (3)$$

图 3 为模型计算结果。从图可以看出，荷电颗粒形成的颗粒层结构比较均匀。

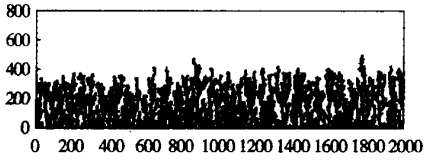

图 3 10 000 个颗粒形成的荷电颗粒层

2 荷电颗粒的可压缩性颗粒层模型

在荷电颗粒形成颗粒层的基础上，继承中和颗粒的可压缩性颗粒层模型，建立荷电颗粒可压缩模型。

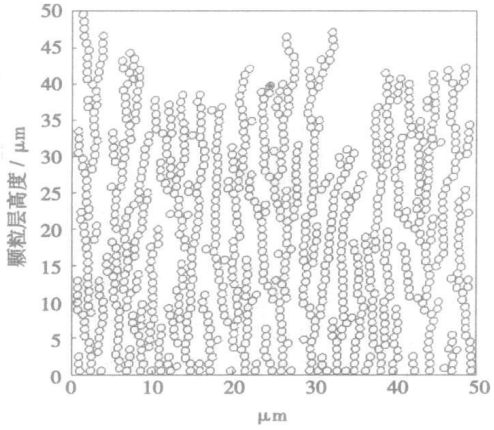

图 4 荷电颗粒层坍塌发生较少时的情况，颗粒数为 1 000，$A = 6\times10^{-20}$，$\tan^{-1}\varphi = 0.2$，$U = 3.95$ m/min

图 4 和图 5 是荷电颗粒形成的颗粒层，其中：A—求范得华力所用的 Hamaker 常数[4]；$\tan^{-1}\varphi$—颗粒的摩擦系数；U—表观过滤速度。为了表示方便，采用过高的速度以便更好地描述颗粒层坍塌结果。可以看出，此工况产生的颗粒层，比起中和工况，其空隙率分布较为均匀，没有局部大的空隙。压缩后，虽然与中和相似，形成了底部颗粒的大量增多，但与之不同的是，坍塌的颗粒链虽然遭到了破坏，而其断裂后仍保留了颗粒链片断，所以压缩后的部分颗粒排布也很整齐。

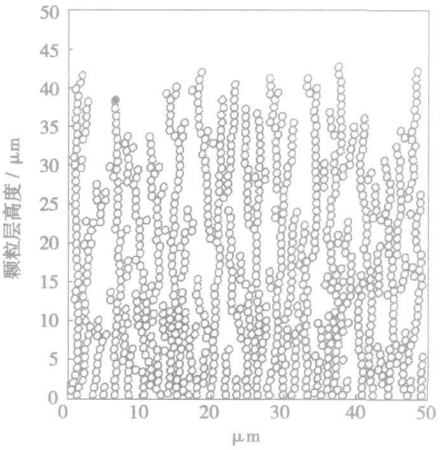

图 5 荷电颗粒层坍塌发生较多时的情况，颗粒为 1 000，$A = 6\times10^{-20}$，$\tan^{-1}\varphi = 0.2$，$U = 39.5$ m/min

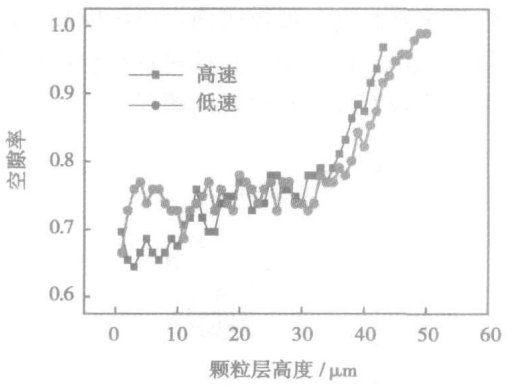

图 6 荷电工况不同过滤速度下颗粒层空隙率，颗粒数为 1 000，$A = 6\times10^{-20}$，$\tan^{-1}\varphi = 0.2$，$U = 3.95$ m/min(低速)，$U = 39.5$ m/min(高速)，$d_p = 1$ μm

图 6 是两个过滤速度下的空隙率情况。与中和相似，荷电颗粒低速时在初始阶段有个小的空隙率，在 0.70～0.75 间保持较稳定到颗粒层高度在 30 μm 左右，然后空隙率从 0.75 增长到 1。高速工况时在 0～10 μm 阶段空隙率在 0.65～0.70 之间，而 10～30 μm阶段则保持在 0.70～0.75 之间。30 μm 之后

与低速相似地从 0.75 增长到 1。颗粒层高度从 50 μm 压缩到 43 μm, 压缩率仅为 14%, 远低于中和工况的压缩效果。这主要是因为荷电工况颗粒与颗粒接触点法线与铅垂线的夹角比起中和工况小造成的。

图 7 是两种流速下颗粒层压降增长的趋势。对于高速情况, 当沉积颗粒超过 500 个以后, 开始出现频繁的压降"跳跃", 不同于中和工况, 这种"跳跃"有着一定的周期性, 这与实验结果相似[3]。

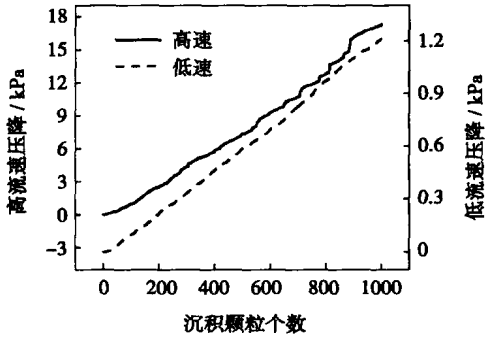

图 7　荷电工况不同过滤速度下颗粒层压降, 颗粒数为 1 000, $A=6\times10^{-20}$, $\tan^{-1}\varphi=0.2$, $U=3.95$ m/min(低速), $U=39.5$ m/min(高速), $d_p=1$ μm

3　荷电和中和颗粒的颗粒层比较

图 8 和图 9 是两工况颗粒层不可压缩和可压缩的空隙率对比。在低速工况, 颗粒层下部(35 μm 以下)空隙率总的趋势相对水平, 虽然两工况在此保持

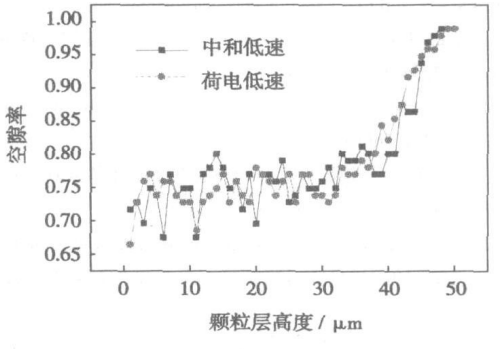

图 8　低速过滤下的空隙率

空隙率相似, 但明显可以看出, 荷电工况的空隙率波动较少, 这说明其空隙分布较为均匀; 而中和工况在此阶段的波动幅度相对更大, 这种局部不均匀的分布将会使总的过滤压降变得较高。对于颗粒层上部, 颗粒空隙率变化相似, 其颗粒层的高度也相近。对于高速工况, 中和颗粒受到压缩坍塌的影响明显大于荷电工况, 除了上部 15 μm 左右比较相似外, 中和颗粒层下部已经有了显著的压缩, 使得空隙率比荷电的小很多。

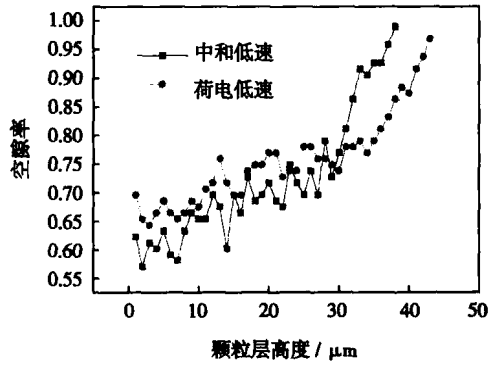

图 9　高速过滤下的空隙率

图 10 和图 11 是两工况下压降增长率的对比。低速压缩较少情况下, 荷电颗粒的压降比中和工况

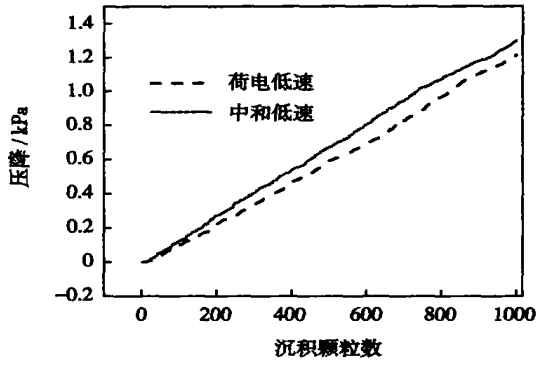

图 10　低速过滤下的压降增长

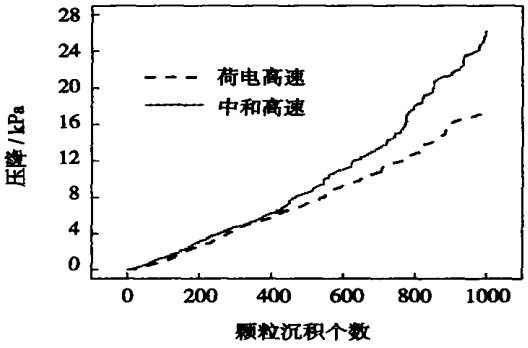

图 11　高速过滤下的压降增长

要小，但相差不显著，这与实验结论是一致的。另外，此处在计算压降时采用了同样的 Kozeny-Carman 常数[5]，由颗粒层结构可以看出，气流在荷电工况中有更直的分布和更好的“管道”流通，其系数应该比中和更低，也就是说，实际过程的荷电压降应该更低。从空隙率的分析可以知道，这是颗粒层空隙率局部分布均匀性造成的。高速工况对比发现，由于中和颗粒更容易坍塌，所以中和工况压降在坍塌影响下更是远大于中和工况。另外，中和的沉积模型简化了由于绕流产生的影响，使得空隙率相对来说比实际还有所增大，所以压降比起实际来说两工况应该有更大的差距。

4 实验中的颗粒层压缩现象

实验过程中颗粒层出现压缩现象最直观的表现是过滤过程中，上下游的压降出现压力陡增现象，由于颗粒层的坍塌造成局部填充率突然增高造成。图 12 和图 13 是覆膜滤料过滤实验过程中电晕荷电和中和工况下压降随着过滤过程增高的曲线。从曲线的结果看出，电晕工况曲线中，当压降增加到一定的时候，颗粒层开始出现周期性的、幅度较大的压降陡增现象；而对于中和工况，这种现象出现得更早更为频繁，但其产生的压降增幅却远小于电晕荷电工况。在低速时，电晕工况和中和工况相差不大，然而，当过滤速度增加后，中和的压降显著大于电晕荷电阶段，这与模拟结果相同。

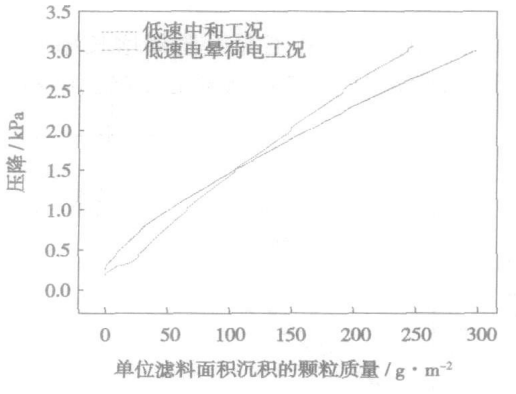

图 12 低速过滤下的压降增长实验曲线

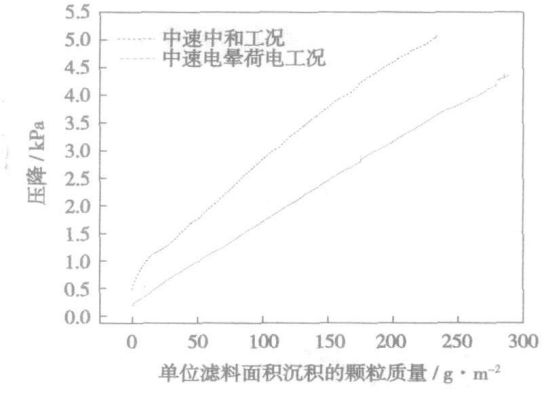

图 13 中速过滤下的压降增长实验曲线

5 结 论

通过引入实验中观察到荷电颗粒沉积的特点，在中和颗粒层的基础上建立了荷电颗粒层形成和坍塌模型，通过模型计算，很好地解释了荷电颗粒层的过滤现象：

（1）荷电颗粒形成分布均匀的颗粒层，与中和工况相比其空隙率波动较小，形成的颗粒层高度虽与中和颗粒层相似，其压降却小于中和工况；

（2）荷电颗粒层由于下滑角小，不易被压缩；压缩后颗粒层过滤压降呈周期性跳跃；在较高的压降下，由于中和颗粒层大幅度压缩，导致了荷电颗粒层过滤压降远小于中和工况。

以上结论与实验结果相似，成功地预测了荷电颗粒层过滤的情况，有利于深入地理解荷电颗粒的过滤过程。

参考文献：

[1] HUANG B, YAO Q. Experimental investigation on the particle capture by a single fiber using microscopic image technique[J]. Powder Technology, 2006, 163(3): 125—133.

[2] CROSS J. Electrostatics: principles, problems and applications[M]. Bristol: Adam Hilger, 1987.

[3] 黄 斌. 静电对过滤可吸入颗粒物的影响研究[D]. 北京：清华大学，2006.

[4] ZENG X M, MARTIN G. Particulate interaction in dry powder formulation for inhalation[M]. London and New York: Taylor & Francis, Limited, 2001.

[5] NEIVA A, LEONARDOA J. A procedure for calculating pressure drop during the build-up of dust filter cakes[J]. Chemical Engineering and Processing, 2003, 42(6): 495—501.

（编辑 渠 源）

热工多变量动态过程主导因素的确定＝**Determination of Major Factors Influencing the Dynamic Process of Thermodynamic Multivariables**[刊, 汉] /ZHANG Xiao-tao, WANG Ai-jun, WANG Ji-dong (College of Electric Power under the North China University of Water Conservancy and Hydropower, Zhengzhou, China, Post Code: 450008), NI Wei-dou (Thermal Energy Department of the Tsinghua University, Beijing, China, Post Code: 100084)// Journal of Engineering for Thermal Energy & Power. —2007, 22(4). —414 ~417

The multivariate statistical analysis can be applied to the monitoring and control of a process. The main variant analytic method and multivariable statistical calculation can be used to determine the major factors influencing the dynamic process of thermodynamic multivariables. In the light of the operating mechanism of a machine unit, the relevant process variables that cause a change of the main monitoring and control variables were determined, the operating data of the relevant process variables collected, and data input matrix and main variant model established. Moreover, T^2 statistical amount and control thresholds were calculated with the contributions of various corresponding process variables to the main variant being computed when T^2 is at its maximal value. The major factors causing a change of the main monitoring and control variables during the operation of the machine unit were determined, which has created a favorable condition for the dynamic modeling of the thermodynamic process and the conduct of fault diagnosis. **Key words**: on-site data, dynamic process, main variant analysis, multivariable statistics, major factor

中储式钢球磨制粉系统的自适应模糊控制＝**Self-adaptive Fuzzy Control of a Ball-mill-based Bin and Feeder System**[刊, 汉] / LU Jian-hong, GUO Ying, WU Ke (Power Department of the Southeast University, Nanjing, China, Post Code: 210096), WANG Xi-ping, et al (Minhang Power Plant, Shanghai, China, Post Code: 200240)// Journal of Engineering for Thermal Energy & Power. —2007, 22(4). —418 ~422

Taking account of the specific features of the ball-mill-based bin and feeder system of No. 11 boiler at Minhang Power Plant and on the basis of the multivariable control theory, fuzzy control and self-adaptive optimization theory with due consideration of characteristics of the mill system, presented were the practical control tactics based on different control theories and control sub-systems incorporating relatively independent functions. The foregoing was proposed after having taken into account the concrete peculiarities of different controlled processes. Then, through an integration of various control subsystems, a full-load optimized control of the whole mill system was accomplished. The control method proposed by the authors has been successfully used in the control of the mill system of No. 11 boiler at Minhang Power Plant since Mar. 2003, thereby not only ensuring a long-term and reliable operation of the mill system but also enabling it to work at its optimum operating condition with notable economic benefits being attained. **Key words**: milling system, ball mill, fuzzy control, self-adaptive optimization, multivariable system

叶片转动角度对百叶窗浓缩器性能影响的研究＝**A Study of the Effect of Blade Rotating Angles on the Performance of a Louver Concentrator**[刊, 汉] / SUN Shao-zeng, WANG Zhi-qiang, JIANG Wen-long, et al (Combustion Engineering Institute under Harbin Institute of Technology, Harbin, China, Post Code: 150001)// Journal of Engineering for Thermal Energy & Power. —2007, 22(4). —423 ~426

By making use of a louver concentrator test system, a study was conducted of the effect of rotating angles of blades in five stages on the performance parameters of the concentrator (dense-thin air ratio R_1, resistance loss coefficient D and average concentration rate R_2). Through an analysis of test results of blades in various stages rotating at different angles, obtained was a change of the performance parameters caused by the variation of blade rotating angles. Regarding the rotating angles of blades in various stages, the operating condition corresponding to a maximal resistance coefficient was found to be one when all the blades in the fifth stage are rotating at 30 degrees. The operating condition featuring a maximal dense-thin air ratio was one in which the blades in the first to fourth stage are rotating at 30 degrees while the blades in the fifth stage at 20 degrees. The operating condition corresponding to a maximal concentration rate was one when all the blades in the fifth stage are rotating at 30 degrees. **Key words**: louver concentrator, dense-thin air ratio, resistance loss coefficient, average concentration rate

荷电颗粒可压缩性颗粒层模型＝**A Model for a Compressible Particle Layer of Charged Particles**[刊, 汉] / HUANG Bin, YAO Qiang, IONG Zheng-wei, et al (Education Ministry Key Laboratory on Thermal Power Engineering and

Thermal Science, Tsinghua University, Beijing, China, Post Code: 100084)// Journal of Engineering for Thermal Energy & Power. —2007, 22(4). —427 ~430

Authors' research has shown that charged particles tend to deposit at the tip of particle chains. On this basis, by adding the deposition properties of charged particles to an already established model of a neutralized compressible particle layer, a model for a compressible particle layer of charged particles was set up. Studied thereupon is the mechanism of the filtration stage of the particle layer during the filtration process of filtering materials. It has been found through the model that in case of incompressiblity, the height of the particle layer formed by charged particles is similar to that of the neutralized particle layer. The distribution of voids, however, is uniform. Owing to the glide angle being relatively small, it is not easy for the above-mentioned layer to be compressed. When the pressure drop is increased to a certain value, the said layer assumes a periodic compression. Therefore, its pressure drop at a relatively high filtering air speed is notably lower than that at the neutralized working conditions. The results obtained from the model can successfully explain the experimental phenomena. **Key words**: charged particle, particle layer, compression, pressure drop, void ratio

干煤粉加压气流床气化试验研究= **An Experimental Study of Dry Pulverized-coal Gasification in a Pressurized Airflow Bed**[刊, 汉] /REN Yong-qiang (College of Energy Source and Power Engineering under the Xi' an Jiaotong University, Xi' an, China, Post Code: 710049), XU Shi-sen, XIA Jun-cang, LI Xiao-yu (Xi' an Thermodynamics Academy Co. Ltd., Xi' an, China, Post Code: 710032)// Journal of Engineering for Thermal Energy & Power. —2007, 22(4). —431 ~434

Described are the main equipment, process flow path and the selection of technological conditions for the gasification pilot plant of a 36 t/d pressurized airflow bed. Also given are the main test data obtained for a multitude of coal ranks undergone experimental research under the condition of the gasification pressure being 3.0 MPa and dry pulverized coal fed being 1 t/h. As can be seen from the test data, the indexes of dry-method gasification are obviously better than those of coal-slurry gasification, mainly due to a low CO_2 content and a high content of effective constituents $CO+H_2$ (both greater than 89%). The foregoing demonstrates the superiority of the dry pulverized coal gasification. The tests have basically achieved the anticipated aim and accumulated relevant data for dry pulverized coal gasification in an airflow bed. **Key words**: coal gasification, airflow bed, dry-feed of raw materials

非均匀受热管管壁温度场的数值计算= **Numerical Calculation of Temperature Fields on a Non-uniformly Heated Tube Wall**[刊, 汉] /WANG Wei-shu, XU Wei-hui (College of Electric Power under the North China Institute of Water Conservancy and Hydroelectric Power, Zhengzhou, China, Post Code: 450008), CHEN Ting-kuan, LUO Yu-shan (National Key Laboratory on Multiphase Flow in Power Engineering under the Xi' an Jiaotong University, Xi' an, China, Post Code: 710049)// Journal of Engineering for Thermal Energy & Power. —2007, 22(4). —435 ~439

In the light of the non-uniform distribution of thermodynamic parameters, such as circumferential wall temperature of the non-uniformly heated tube wall and heat load etc., a two-dimensional mathematical model was established for simulating and calculating the temperature field of a non-uniformly heated tube with the outer wall temperature and heat-dispersion thermal load serving as boundary conditions. Based on the idea of radial node advancement, the authors have adopted a finite volume method to set up a discrete equation. A numerical calculation program was prepared to solve the reverse problem of heat conduction in the two-dimensional temperature field on the non-uniformly heated tubes determined by the coupling of the fluid heat exchange and tube wall heat conduction. By making use of the program, calculated was the heat transfer characteristics of semi-circle heated vertical riser (bare tube $\phi 32\times 3$ mm and $\phi 24\times 4$ mm) with respect to supercritical water. The calculation results can exceedingly well reflect the wall temperature distribution regularity of non-uniformly heated tubes and exhibit a good computation convergence. The results of calculation also indicate that at a supercritical pressure, the semi-circle heated vertical bare-riser wall temperature and wall surface heat load assume a non-uniform circumferential distribution. The side with a high heat load has a high temperature and the side with a low heat load a low temperature. In the pseudocritical zone, a heat transfer intensification occurs and an increase of in-tube heat transfer coefficient will weaken the flow-equalizing role of heat along the circumferential direction of tube walls. **Key words**: temperature field, reverse problem of heat conduction, heat load, non-uniformly heated tube